

## Heat capacity and thermal conductivity of granular Al-Ge

Y. Shapira and G. Deutscher

*Department of Physics and Astronomy, Tel Aviv University, Tel Aviv 69978, Israel*

(Received 1 August 1983; revised manuscript received 30 November 1983)

We have measured the heat capacity and thermal conductivity of films of granular Al-Ge. There is no evidence for a change in the electronic specific heat capacity, but the lattice heat capacity is much greater than that of the constituents. The superconducting transitions of these films are also studied.

## I. INTRODUCTION

Granular Al-Ge consists of metallic Al grains embedded in an amorphous Ge matrix.<sup>1,2</sup> Based on electron-microscope data the Al-Ge is characterized by a grain size ( $d \sim 120$  Å) (Refs. 1 and 2) which is much larger than that of similar systems, i.e., Al-Al<sub>2</sub>O<sub>3</sub> ( $d \sim 30$  Å).<sup>3</sup> While in Al-Al<sub>2</sub>O<sub>3</sub> the grain size is such that thermodynamic fluctuations prevent the existence of bulk superconductivity when they are isolated. We can expect to observe some single-grain superconducting properties in Al-Ge.

In this paper we describe heat-capacity and thermal-conductivity measurements of some Al-Ge specimens. From the normal-state heat-capacity data we see no evidence for a change in the electronic specific heat capacity of the Al grains, while the lattice heat capacity is significantly larger than that of the same bulk constituents. A similar phenomenon was found for Al-Al<sub>2</sub>O<sub>3</sub> (Ref. 4). In general, the heat-capacity and thermal-conductivity results for Al-Ge resemble those of Al-Al<sub>2</sub>O<sub>3</sub>, including the thermal conductivity at high metal concentrations, the absence of a clear superconducting transition in the thermal conductivity, and the shape of the heat-capacity transition. However, some characteristics of single-grain behavior are observed in the heat-capacity transition for the Al-Ge system.

## II. SPECIMENS

The specimens were prepared by coevaporation of Al and Ge from two electron-beam guns. The substrate is water-cooled at room temperature and is placed above the guns. The substrates are a 70- $\mu$ m-thick glass 0211 Corning Microsheet. The total thickness of each constituent is measured independently by a Kronon QM-311 thickness

monitor, and the output of the monitor is fed into a controller to help stabilize the evaporation rate. The combined rate of both guns is 30–50 Å/sec. The vacuum is kept at  $1-2 \times 10^{-6}$  Torr during evaporation. The substrates are mounted along the line connecting the center of the guns and are perpendicular to that line. Using this procedure we obtain during each evaporation four samples  $4 \times 1$  cm each with a 3–4 % change of metal volume concentration from sample to sample. A thermometer and a heater are attached to the sample by 7031 General Electric varnish: the heater at one end of the sample, the thermometer in the middle, while the other side is attached to a copper block. The heater is prepared by evaporating 700-Å-thick Kental<sup>5</sup> (72 at. % Fe, 20 at. % Cr, 6 at. % Al, 2 at. % Ca) on a 7- $\mu$ m nylon sheet. The thermometer is prepared by grinding a 370- $\Omega$  Speer resistor until its mass is reduced to less than 1 mg and its resistance enhanced by a factor of 5–10. The contact leads<sup>6</sup> are 0.001 25-in. Au wires with 7 at. % of Cu (California fine wire company). The configuration of the specimen was discussed elsewhere.<sup>4,7,8</sup>

The thickness of the evaporated film is about 10  $\mu$ m. Table I gives the principal parameters of all the samples investigated in this study. As can be seen the study concentrates on low metal concentrations with only one sample with high metal concentration and high normal-state conductivity.

## III. EXPERIMENTAL

The heat capacity and thermal conductivity were determined by a heat-pulse method which was described elsewhere.<sup>1,3,5,6</sup> The experimental system is composed of an externally triggered function generator, model HR-8 Princeton Applied Research lock-in amplifier, and a Digital

TABLE I. Parameters for the heat-capacity samples:  $d$  is the thickness of constituents Al and Ge;  $c$  is the metal volume concentration.  $\rho_n$  is the normal-state resistivity at RT (room temperature) and LH (liquid-helium) temperatures.  $T_{ce}$  is the electrical superconducting transition.

Sample	$d_{Al}$ ( $10^3$ Å)	$d_{Ge}$ ( $10^3$ Å)	$C$	$\rho_n$ (RT) ( $\mu\Omega$ cm)	$\rho_n$ (LH) ( $\mu\Omega$ cm)	$T_{ce}$ (K)
A	Typical	Glass	Substrate			
B	74.3	14.5	0.85	24	11.2	1.60
C	66.4	35.1	0.66	5050	6310	1.65
D	52.1	44.9	0.54	29 100	46 100	

Equipment Corporation PDP-8 computer with a storage scope. Characteristic values of the temperature excursion  $\Delta T$  of the thermometer are 10 mK at 0.9 K and 20 mK at 2 K with  $10^{-8}$  and  $5 \times 10^{-8}$  J, correspondingly, for the energy of the heat pulse. The measuring time is dependent on the diffusivity  $D$  and ranges from 0.3 sec at low temperatures to few seconds at 4 K.

We have used the heat-pulse technique<sup>5,7</sup> since it enables us to measure the heat capacity and the thermal conductivity simultaneously. As will be seen later there is very little unusual physical information in the thermal-conductivity data. Since the only advantage of the heat-pulse method on the ac method<sup>1,9,10</sup> is simultaneous measurement of thermal conductivity, we can summarize, in retrospect, that the ac method would have been more suitable for our purpose.

#### IV. RESULT

In Table I we present the main parameters of the samples which were measured for the purpose of this work. We have calibrated our experimental system by measuring the heat capacity and thermal conductivity of the glass substrates. The agreement between our data and that of others<sup>8</sup> on the same glasses is within experimental error.

Figures 1 and 2 show typical heat-capacity and electrical-conductivity data for samples *B* and *C*, respectively, in the vicinity of the superconducting transition. We can see the raw data and a fit of the form  $C = \gamma T + AT^3 + BT^5$  to the data points above the transition area. The fit is extrapolated to include the transition region.

We can see from Figs. 1 and 2 the reproducibility and scattering of our data points, or the excess of random error due to measuring techniques. From the above figures we estimate the random error to be of the order of 4%.

Since we use some more than 30 experimental points in order to extract bulk quantities, such as the electronic heat capacity out of the data, this error is significantly reduced. However, there are some uncertainties in our measurements which are not of a random nature and are harder to evaluate. These uncertainties include the exact heat capacity of the thermometer, the heat leakage through the measuring wires, calibration of the thickness of the sample, and so on. Although our measuring technique is aimed at reducing some of these uncertainties, it is quite difficult to estimate its exact value. In Table II we present our results for bulk quantities of our samples in the normal state. We estimate the overall uncertainty to be of the order of 5–7%.

Figures 3 and 4 show smoothed curves of  $C/T$  vs  $T^2$  and  $K(T)$  for all the samples. The scattering of the data points for both figures was typical as that seen in Figs. 1 and 2 for similar data. The smoothing procedure was done by the help of a spline function. Note that there is no transition seen in the thermal-conductivity data.

#### V. THERMAL CONDUCTIVITY

As can be seen from Fig. 4, the thermal conductivity for samples *C* and *D* is nearly that of the substrate alone. This indicates that, for those samples, the thermal conductivity of the Al-Ge films is very small. A similar result was obtained for Al-Al<sub>2</sub>O<sub>3</sub> (Ref. 11) films with resistivities higher than 1000  $\mu\Omega$  cm. Assuming the Wiedemann-Franz law<sup>12</sup> to be valid, the high electrical resistivities of samples *C* and *D* are indeed accompanied by a negligible electronic thermal conductivity. One is left with the thermal phonon conductivity which appears to be of the order of the conductivity of the glass substrate, and with negligible contribution of the Al-Ge film. The small contribution of the Al-Ge film compared to the glass is

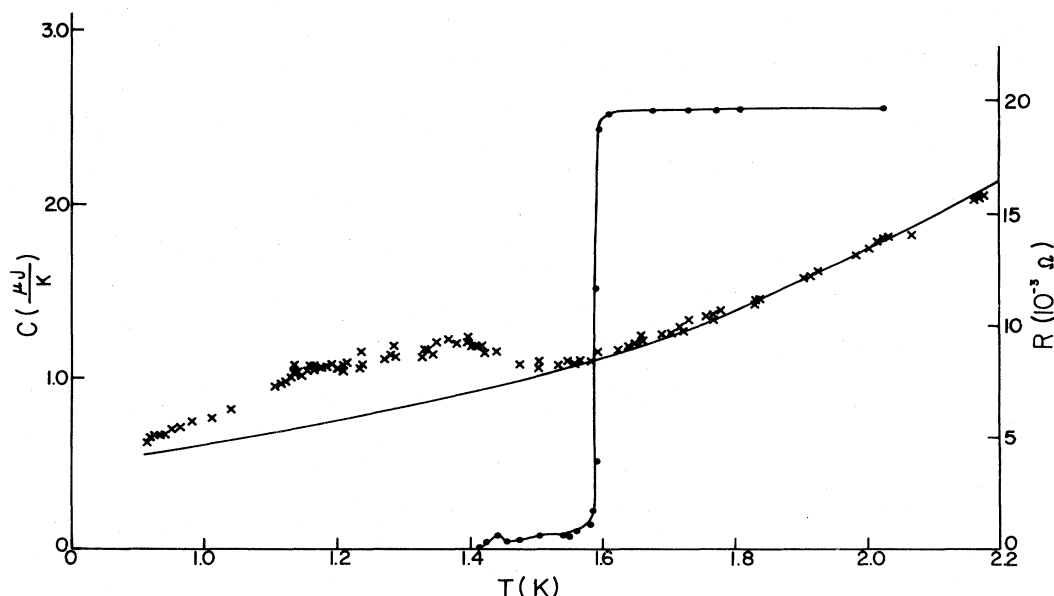


FIG. 1. Heat capacity  $C$  as a function of temperature in the superconducting transition region for sample *B*. The crosses are the data points. The solid line is a best fit of the form  $C = \gamma T + AT^3 + BT^5$  to the data above the transition region. The dots and the solid line connecting them are the electrical transition of that sample.

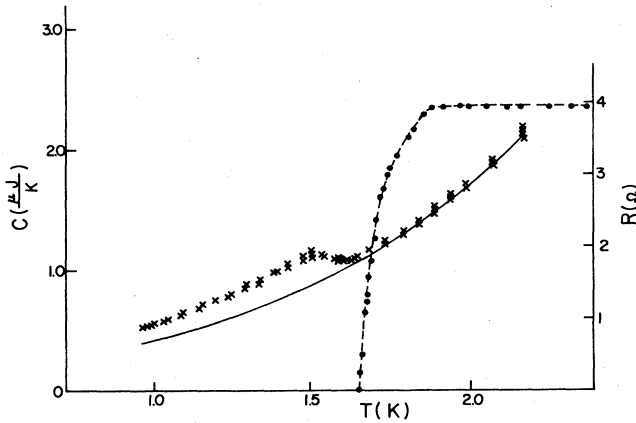


FIG. 2. Heat capacity  $C$  as a function of temperature in the superconducting transition for sample  $C$ . The crosses are the data points. The solid line is a best fit of the form  $C = \gamma T + AT^3 + BT^5$  to the data above the transition region. The circles and the solid line connecting them are the electrical transition of that sample.

explained mainly by the different cross section of the glass and the Al-Ge film.

The thermal conductivity of sample  $B$  is more interesting since it shows a measurable conductance of the Al-Ge sample. It seems reasonable to assume that the phonon conductance is nearly the same for all samples in Fig. 4. In that case, the difference between the thermal conductance of samples  $B$  and  $A$  must be mostly electronic, and the Wiedemann-Franz law can be checked for sample  $B$ . The law states that

$$L_0 = \frac{K\rho_0}{T}$$

with  $L_0 = 2.45 \times 10^{-8} \text{ V}^2/\text{K}^2$  is a universal constant often called the ideal Lorenz number,  $\rho_0$  is the electrical resistivity,  $K$  is the electronic thermal conductivity, and  $T$  is the temperature. From Fig. 4 and Table I we indeed find a linear dependence of the electronic contribution to the thermal conductivity versus  $T$  and calculate  $L = 1.8L_0$ . The same value of  $L/L_0$  was found for Al-Al<sub>2</sub>O<sub>3</sub> (Ref. 11) samples with high thermal conductivity. We do not know at this stage whether this agreement is coincidental or rather indicates a systematic deviation from the Wiedemann-Franz law in granular metals.

It is quite unexpected that no superconducting transition was seen in sample  $B$ , despite its high electronic thermal conductivity. The same was found for Al-Al<sub>2</sub>O<sub>3</sub> samples. We have no explanation for that observation.

## VI. HEAT CAPACITY

The heat capacity is the sum of the electronic term and the phonon term

$$C = \gamma T + AT^3,$$

where  $\gamma = \frac{1}{3}\pi^2 N(0)k_B^2 T$  and  $A = 12\pi^4 R/5\Theta_D^3$ .  $N(0)$  is the density of states at the Fermi level,  $\Theta_D$  is the Debye temperature.

Figure 5 shows a smooth plot of  $C/T$  as a function of  $T^2$  for samples  $B$ – $D$  after subtraction of the heat capacity of the substrate. From values of the intercepts and slopes we calculate  $N(0)$  and  $\Theta_D$  and reach the following conclusions.

(i) The density of electronic state  $N(0)$  is, within experimental accuracy, that of the Al metal in the sample. The same conclusion was reached for Al-Al<sub>2</sub>O<sub>3</sub> (Ref. 5) samples. According to the theory of strong coupling superconductors  $\gamma$  is larger than the band-structure value by the factor  $(1 + \lambda)$ , where  $\lambda$  is the electron-phonon coupling parameter. For the enhancement we observed, according to McMillan,<sup>13</sup> we would predict, at least for the superconducting samples ( $B$  and  $C$ ) an increase in  $\gamma$  by 7% over the value for bulk Al. In Table II we present our results for  $\gamma$  as compared to  $0.174 \times 10^{23}$  states/eV cm<sup>3</sup> of bulk Al. Unfortunately, our experimental accuracy is not sufficiently good to check the validity of the above theory.

(ii) As can be seen from Table II, the measured value of  $A$  turned out to be much larger than that calculated for the sum of constituents, assuming bulk values of  $\Theta_D$  for Al ( $\Theta_D = 426$  K) and for Ge ( $\Theta_D = 370$  K). That phenomenon could be attributed to a decrease in  $\Theta_D$  of either the Al or the Ge or both. Similar results were obtained for Al-Al<sub>2</sub>O<sub>3</sub> samples,<sup>4,6</sup> and have been attributed to a softening of surface phonons in the Al grains,<sup>6</sup> or to the amorphous structure of the insulator.<sup>4</sup> The situation for other granular materials is not clear and while for some of them, i.e., Ag, Al, V, and Pd (Refs. 14 and 15) the softening is great and of the order we obtained; however, for others, i.e., Pb, In, and Sm (Refs. 16 and 17) it is nearly absent. A full review of all the relevant experimental results is presented in Refs. 4 and 5. We suspect that the decrease in  $\Theta_D$  is caused by the granular structure and is absent for random metal-insulator mixtures. Yet there is not enough experimental structural evidence to check the validity of that assumption.

By assuming that the Debye temperature of Ge retains its bulk value, our data for Al yields  $\Theta_D = 280 \pm 20$  K for all samples  $B$ – $D$ . This value is similar to that obtained in Ref. 6 ( $\Theta_D = 300$  K) for two Al-Al<sub>2</sub>O<sub>3</sub> samples with different Al concentrations. Despite the great difference in grain size between the Al-Ge grains ( $d \sim 120$ ) (Ref. 1) and

TABLE II. Results obtained from heat-capacity measurements in the normal state.  $c$  is the metal volume concentration;  $\gamma$  and  $A$  are the electronic and the phonon terms, respectively, of the heat capacity.

Sample	$C$	$\gamma$ ( $10^{23}$ states/eV cm <sup>3</sup> )	$A$ measured ( $10^{-3}$ $\mu\text{J}/\text{K}^4$ )	$A$ computed ( $10^{-3}$ $\mu\text{J}/\text{K}^4$ )
$B$	0.85	0.181	15.6	4.32
$C$	0.66	0.172	10.75	5.05
$D$	0.54	0.165	12.0	4.55

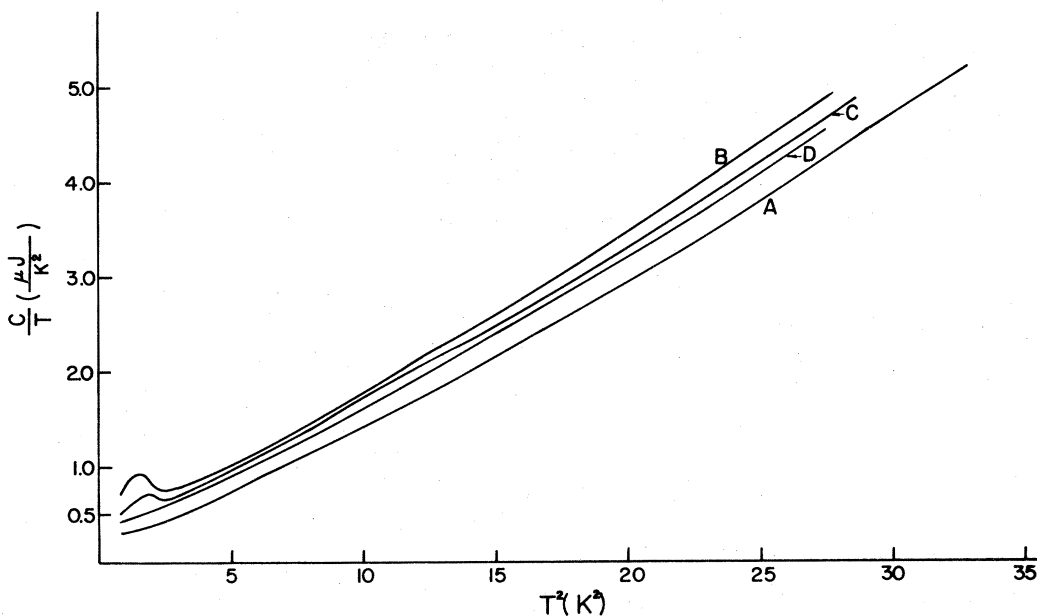


FIG. 3.  $C/T$  as a smoothed function of  $T^2$  for samples  $A-D$ .

the Al- $\text{Al}_2\text{O}_3$  grains ( $d \sim 30 \text{ \AA}$ ) (Ref. 3),  $\Theta_D$  is nearly the same for both systems.

It is known that amorphous Ge has a lower  $\Theta_D$  than crystalline Ge.<sup>18,19</sup>  $\Theta_D$  is found to be  $315 \pm 5 \text{ K}$  for amorphous Ge (Ref. 18) as compared to  $370 \text{ K}$  of the crystalline phase. Moreover, we would expect in the temperature range of interest a further decrease of about 5% in  $\Theta_D$  as  $\Theta_D$  at  $6 \text{ K}$  is about 0.9 of  $\Theta_D$  at  $T=0 \text{ K}$ .<sup>18</sup> Using the value of  $\Theta_D=315 \text{ K}$  for the Ge in our samples and repeating the above procedure we obtain  $\Theta_D=300 \text{ K}$  for the Al grains but with great variance between the various samples.

We have tried to attribute all the change in the heat capacity to the Ge matrix. We have found for samples  $C$

and  $D$  that  $(\Theta_D)_{\text{Ge}}=230 \text{ K}$  while, for sample  $B$ ,  $\Theta_D=150 \text{ K}$ . These figures are quite low compared to  $\Theta_D$  of  $315 \text{ K}$  for amorphous Ge, even if we take into account an additional decrease in the temperature range of interest.<sup>18</sup> We can understand such low figures only by taking into account that the Ge is built in the form of very thin layers which are of the order of  $10 \text{ \AA}$  for samples  $C$  and  $D$  and the order of  $3 \text{ \AA}$ , or one monolayer, for sample  $B$ .<sup>20</sup> For such thin films we would expect a drastic change in some physical behavior. Such a change was seen for very thin Pb films sandwiched between Ge films,<sup>21</sup> where for very thin films the melting point was considerably reduced. If a reduction of the melting temperature can be attributed to softening of the elastic constants, then we would expect,

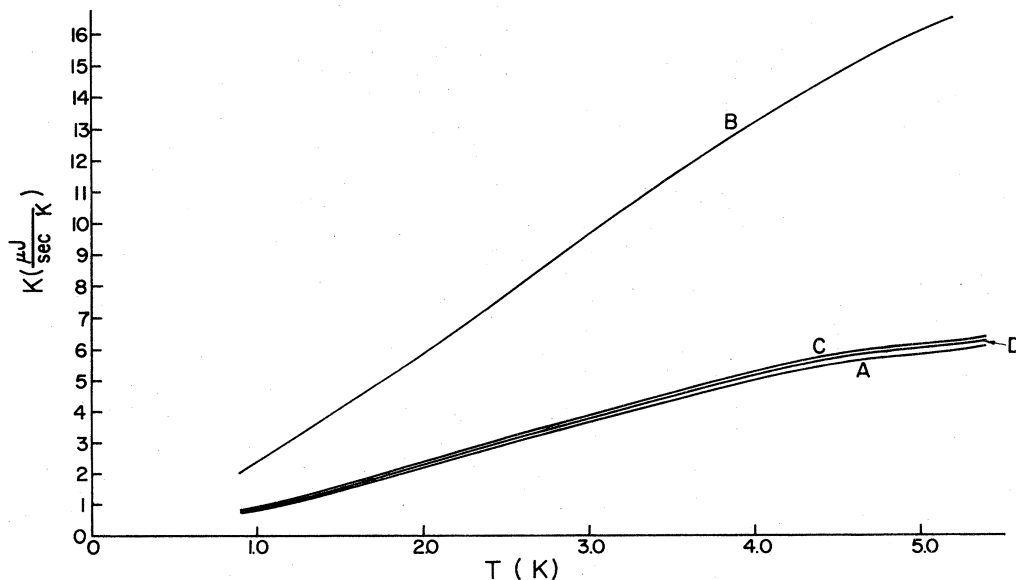


FIG. 4. Thermal conductivity  $K$  as a function of temperature for samples  $A-D$ .

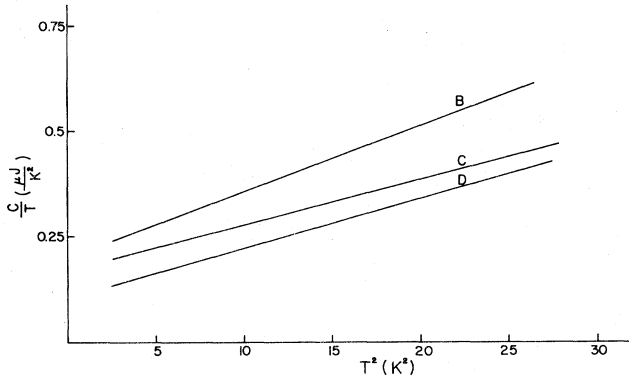


FIG. 5.  $C/T$  as a smoothed function of  $T^2$  for samples  $B-D$  after subtracting the heat capacity of the substrate.

also, a decrease in  $\Theta_D$ , which would be much larger for a thickness of the order of one monolayer.

It seems that we must attribute the change in  $\Theta_D$  both to the Al grains and the Ge matrix and it is hard to conclude which contribution is the largest. But considering the relatively large grain size and the thin amorphous films, it seems more plausible that the Ge undergoes a more drastic change, at least as far as the phonon spectrum is concerned, and that surface phonons are responsible for the softening of  $\Theta_D$ .

## VII. SUPERCONDUCTING TRANSITIONS

Samples  $B$  and  $C$  show a superconducting transition in the heat-capacity data. The most convenient representation of the data is through the ratio  $C_{es}/C_{en}$  where  $C_{es}$  and  $C_{en}$  are the electronic heat capacity in the superconducting state and the normal state, respectively.

In order to obtain  $C_{es}$  we have fitted the data, above the transition, to a polynome of odd powers of  $T$ . Using that fit we could extrapolate our data in the normal state down to the superconducting state as seen in Figs. 1 and 2. The difference between the data and the above extrapolation is  $C_{es} - C_{en}$ . We could use an alternative procedure by using the values of  $\gamma$  and  $A$  obtained in the preceding section to obtain an extrapolation of the normal-state data to the superconducting state. We find no difference between the results of the two procedures. For  $C_{en}$  we have used the value of  $\gamma$  obtained from the normal-state heat capacity as described in the preceding section. Using the above procedure we have obtained the temperature variation of  $C_{es}/C_{en}$  for samples  $B$  (Fig. 6) and  $C$  (Fig. 7).

In order to estimate if the superconducting transition is a bulk property or a surface phenomenon, we must compare entropies. This was done first by extrapolating the data in Figs. 6 and 7 to  $T=0$  K, where in Fig. 6 it was done by using at low temperatures a fit of the form of the BCS transition, and in Fig. 7, by extrapolating the results of the model described later.<sup>22</sup> For low temperatures, the model coincides with a BCS transition.<sup>22</sup>

From inspection of Figs. 6 and 7 we can see that the area under the heat-capacity curve in the superconducting state is of the order of the respective transition in the heat

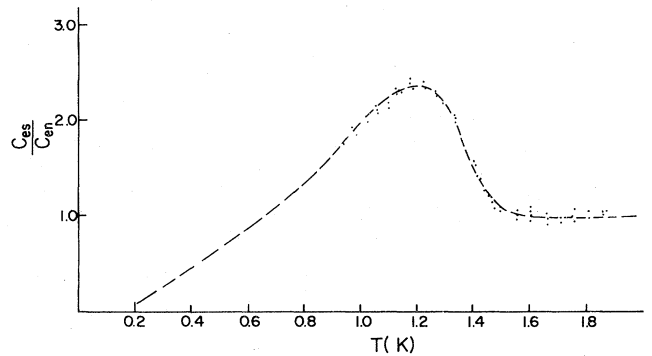


FIG. 6.  $C_{es}/C_{en}$  as a function of temperature for sample  $B$ . The dashed line is an extrapolation of the data down to  $T=0$ .

capacity. Of course, our data are not sufficient to allow us a precise comparison, but we can conclude that the superconducting transition is a bulk property and not a surface phenomenon, and at least most of the sample becomes superconducting in the transition. The same conclusion was obtained for Al-Al<sub>2</sub>O<sub>3</sub> for smaller (30 Å) grain size.<sup>8</sup>

It was already pointed out<sup>4,23</sup> for Al-Al<sub>2</sub>O<sub>3</sub> samples that the Mühlshlegel, Scalapino, and Denton (MSD) theory<sup>24</sup> for a single grain does not properly explain heat-capacity results for coupled grains. We have developed elsewhere<sup>22</sup> a percolation model in order to take coupling between grains into account. The above model was found to explain properly the heat-capacity results for Al-Al<sub>2</sub>O<sub>3</sub> (Ref. 22). It is of interest to compare this model to our Al-Ge samples since, due to the small grain size in Al-Al<sub>2</sub>O<sub>3</sub>, there is practically no contribution from the single-grain properties to the heat capacity, while for Al-Ge we can expect to observe that contribution.

The above percolation model is not valid in the range of low resistivities and high metal concentrations. In this region the principal parameter is the change of  $T_c$  of the single grain as a function of grain size. For samples with low resistivities and narrow distribution of grain sizes, we would expect a BCS behavior. For a wide distribution of grain size we would expect to obtain some type of a smeared transition with a width that is governed by the width of the distribution. Granular materials usually have a wide distribution of grain sizes for low normal-state resistivities<sup>3</sup> and indeed we can see for sample  $B$ , in Fig. 6, a smeared transition with a height of about the BCS jump of 1.47. The same was observed by others for Al-Al<sub>2</sub>O<sub>3</sub> samples.<sup>6,8</sup> When the transition is smeared we would expect the height of the specific-heat jump at the transition to be somewhat less than the BCS jump. The experimental accuracy of our result does not let us distinguish the difference.

The case of sample  $C$  is quite different since its resistance is within the range of validity of the model.<sup>22</sup> Since we have only one sample in that range we did not use any adjustable parameters in order to compare the experimental results with theory, except for the transition temperature,  $T_c$ , which is not given by the model and is merely a shift of the results on the temperature axis.

Figure 7 is a plot of the experimental data points compared to a calculation based on the above-mentioned

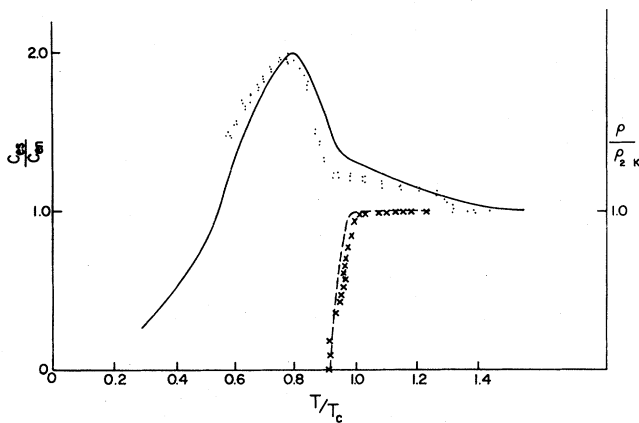


FIG. 7.  $C_{es}/C_{en}$  as a function of  $T/T_c$  for sample *C* with  $T_c = 1.8$  K. The points are the data points while the solid line is the calculation based on the model presented in the text (after Ref. 22). The dashed line is the electrical transition of the same model. The crosses are the experimental points of the electrical transition normalized to the resistance at 2 K.

model with  $T_c = 1.8$  K. The model involves the use of two parameters: the grain's size and the width of the distribution of the junction resistances between neighboring grains. Since the width of the distribution cannot be measured experimentally it may be obtained by fitting the theory to the heat-capacity data. We have chosen not to make any fits to the data but rather used the values obtained as a fit for Al-Al<sub>2</sub>O<sub>3</sub> samples,<sup>22</sup> which was found to have a standard deviation of 0.6 of the mean value of the

distribution. The grain's size affects the calculation by two different modes. Once, indirectly, by calculating the mean junction resistance out of the normal-state resistivity,<sup>22</sup> and the second time, directly, by the heat capacity of the single grain,<sup>24</sup> which for small grains nearly does not contribute to the heat capacity by its own, but the sufficiently large grains<sup>24</sup> have a significant contribution, besides its bulk value when coupled to a big cluster of other grains. This contribution is mainly seen by a tail in the heat capacity for temperatures above  $T_c$ .

The grains' diameter for sample *C*, taking into account its metal volume concentration, was found by electron microscopy to be 120 Å, which yields a  $\delta$  in the MSD theory<sup>22</sup> equal to 0.25. By substituting in the above model for heat capacity<sup>22</sup> of  $\delta = 0.25$  and the normal-state resistivity of sample *C*, the solid line of Fig. 7 was obtained. The fit between experimental data and theory is quite good. The dashed line in Fig. 7 is the electrical transition for the same sample as calculated by the model, while the crosses are the experimental points of the electrical transition. The tail in the specific heat for temperatures above  $T_c$  is easily seen and, as was previously explained, may be attributed to the single-grain limit for such large grains.

The reason for the absence of a superconducting transition in the heat capacity for sample *D* is not fully clear to us since we would expect to be able to see, at least, the single-grain transition. A possible explanation lies in recent measurements of the structure of the Al-Ge mixture with low metal concentration.<sup>25</sup> It was found<sup>25</sup> that, for metal concentrations of the order of sample *D*, the granular structure is replaced by an amorphous mixture of Al and Ge for which we would not expect a superconducting transition.

- <sup>1</sup>G. Deutscher, O. Entin-Wohlman, and Y. Shapira, *Phys. Rev. B* **22**, 4264 (1980).
- <sup>2</sup>G. Deutscher, M. Rappaport, and Z. Ovadyahu, *Solid State Commun.* **28**, 593 (1978).
- <sup>3</sup>G. Deutscher, H. Fenichel, M. Gershenson, E. Grunbaum, and Z. Ovadyahu, *J. Low Temp. Phys.* **10**, 231 (1973).
- <sup>4</sup>R. L. Filler, P. Lindenfeld, T. Worthington, and G. Deutscher, *Phys. Rev. B* **21**, 5031 (1980).
- <sup>5</sup>S. Alterovitz, G. Deutscher, and M. Gershenson, *J. Appl. Phys.* **46**, 3637 (1975).
- <sup>6</sup>R. L. Greene, C. N. King, R. B. Zubeck, and J. J. Hauser, *Phys. Rev. B* **6**, 3297 (1972).
- <sup>7</sup>M. Gershenson and S. Alterovitz, *Appl. Phys.* **5**, 329 (1975).
- <sup>8</sup>R. L. Filler, P. Lindenfeld, and G. Deutscher, *Rev. Sci. Instrum.* **46**, 439 (1975).
- <sup>9</sup>P. F. Sullivan and G. Seidel, *Phys. Rev.* **173**, 679 (1968).
- <sup>10</sup>B. C. Gibson, D. M. Ginsburg, and P. C. Tai, *Phys. Rev. B* **19**, 1409 (1979).
- <sup>11</sup>G. Deutscher, P. Lindenfeld, and R. Filler (unpublished).
- <sup>12</sup>See, e.g., C. Kittel, *Introduction to Solid State Physics* (Wiley, New York, 1968).
- <sup>13</sup>W. L. McMillan, *Phys. Rev.* **167**, 331 (1968).
- <sup>14</sup>G. H. Cosma, D. Haitkamp, and H. S. Rade, *Solid State Commun.* **20**, 877 (1976).
- <sup>15</sup>G. H. Cosma, D. Haitkamp, and H. S. Rade, *Solid State Commun.* **24**, 547 (1977).
- <sup>16</sup>V. Novtony and P. P. Meincke, *Phys. Rev. B* **8**, 4186 (1973).
- <sup>17</sup>S. Akselrod, M. Pasternak, and S. Bukshpan, *Phys. Rev. B* **11**, 1040 (1975).
- <sup>18</sup>C. N. King, W. A. Phillips, and J. P. deNeufville, *Phys. Rev. Lett.* **32**, 538 (1974).
- <sup>19</sup>A. Cruz-Urbe and J. Trefny, in *Proceedings of the Seventh International Conference on Amorphous and Liquid Semiconductors, Edinburgh, Scotland, 1977*, edited by W. E. Spear (Stevenson, Dundee, Scotland, 1977), p. 175.
- <sup>20</sup>Y. Shapira and G. Deutscher, *Thin Solid Films* **87**, 29 (1982).
- <sup>21</sup>R. H. Willens, A. Kornblit, L. R. Testardi, and S. Nakadara, *Phys. Rev. B* **25**, 290 (1982).
- <sup>22</sup>G. Deutscher, O. Entin-Wohlman, S. Fishman, and Y. Shapira, *Phys. Rev. B* **21**, 5041 (1980).
- <sup>23</sup>T. Worthington, P. Lindenfeld, and G. Deutscher, *Phys. Rev. Lett.* **41**, 316 (1978).
- <sup>24</sup>B. Mühlshlegel, D. J. Scalapino, and R. Denton, *Phys. Rev. B* **6**, 1767 (1972).
- <sup>25</sup>A. Kapitulnik, Ph.D. thesis, Tel-Aviv University, 1983.